

Numerical Study of Non-Gray Radiative Heat Transfer in a T-shaped Furnace

Amin Al Taha

Department of Mechanical Engineering,
Kerman Branch, Islamic Azad University, Kerman, Iran
E-mail: mohakeshtkar@gmail.com

Mohammad Mahdi Keshtkar*

Department of Mechanical Engineering,
Kerman Branch, Islamic Azad University, Kerman, Iran
E-mail: mkeshtkar54@yahoo.com

*Corresponding author

Received: 20 October 2019, Revised: 11 January 2020, Accepted: 4 February 2020

Abstract: Radiative heat transfer has an important role in many industrial equipment; i.e. furnaces, boilers and high temperature heat exchangers. In this paper, combination of Weighted Sum of Gray Gas Method (WSSGM) and Discrete Ordinate Method (DOM) are used together in order to numerically study the radiative heat transfer behavior in a non-gray participating medium. Moreover, the concept of Blocked-off region for irregular geometries is used to simulate the T-shaped furnace. The effect of different radiative parameters, i.e. scattering coefficient and wall emissivity on thermal behavior and wall heat fluxes is investigated and compared for both gray and non-gray media. The results show that when scattering coefficient increases, more radiation is scattered in the medium and therefore less heat flux reaches the walls such that by increasing scattering coefficient from 1.0 to 5.0, the incident radiative heat flux decreases up to 15% in some parts of bottom wall. It is seen that by increasing wall emissivity from 0.5 to 1.0, wall heat flux increases more than 60%. Moreover, results show that, by increasing the temperature, the maximum error strongly increases which indicates that in many engineering problems, the gray medium assumption leads to great error in results.

Keywords: Blocked-Off, Discrete Ordinate Method, Non-Gray Media, Radiative Heat Transfer, Weighted Sum of Gray Gas Method

Reference: Amin Al Taha, and Mohammad Mahdi Keshtkar, “Numerical Study of Non-Gray Radiative Heat Transfer in a T-shaped Furnace”, Int J of Advanced Design and Manufacturing Technology, Vol. 13/No. 1, 2020, pp. 39–49.

Biographical notes: **Amin AL-Taha** is a MSc Student in Mechanical Engineering in the Faculty of Engineering, Islamic Azad University, Kerman, Iran. **Mohammad Mahdi Keshtkar** received his PhD in Mechanical Engineering from University of IAU, Science and Research Branch in 2009. He is currently Associate Professor at the Department of Mechanical Engineering, Kerman Branch, Islamic Azad University, Iran.

1 INTRODUCTION

The radiative heat transfer plays an important role in many engineering applications such as combustion systems of furnaces, combustion chamber of the diesel spray in rocket, engine combustion chamber, etc. In order to obtain the radiative thermal behavior of such equipment, Radiative Transfer Equation (RTE) which is an integro-differential equation should be solved numerically. For this purpose, during past decade, many numerical methods have been developed by researchers for solving RTE in gray and non-gray media, i.e., the Discrete Transfer Method (DTM), Zone Method, etc. for gray media and Weighted Sum of Gray Gases coupled with Discrete Ordinate Method (DOM), the Line-By-Line (LBL) model, the Statistical Narrow Band model (SNB), Wide Band Model (WBM) and etc. for non-gray media. Among mentioned numerical methods, DOM is one of the simplest and most widely used methods for simulating radiative heat transfer. Sakami et al. [1] used DOM based on triangular grids ideally suited to complex geometry and the superposition technique. Their results showed the capability of the DOM method with complex geometry. Koo et al. [2] studied DOM for unstructured grid in orthogonal curvilinear coordinates and found acceptable results in terms of medium temperature. In order to reduce the computer calculation for complex geometries, Talukdar [3] used blocked-off method with the Discrete Transfer Method (DTM) for irregular geometries and gray media and obtained accurate results in all situations. Borjinia et al. [4] studied the radiative heat transfer in a 3D complex industrial boiler including five baffles. The boiler was containing a mixture of carbon dioxide and water vapor as a non-gray medium. The blocked-off procedure and WSGG method were used to simulate thermal behavior and radiative heat flux inside the boiler.

Han et al. [5] and Jang et al. [6] studied transient and steady-state thermal behavior of slab in a walking-beam type reheating furnace. The non-gray weighted sum of gray gas model was used for better accurate prediction of gas radiation inside the furnace. Moreover, the block-off procedure was used to simulate the irregularities of the furnace. Keshtkar and Gandjalikhan Nassab [7] studied porous radiant burner under 2-D radiation field by using DOM and found good agreement between theoretical and experimental results. Ansari and Gandjalikhan Nassab [8] studied laminar convective flow of radiating gas in which the DOM combined with blocked-off method were used in order to simulate the thermal behavior over an inclined backward facing step. Abbassi et al. [9] studied radiative heat transfer in a 2D complex geometry biomass pyrolysis reactor. The blocked-off region procedure was used to treat the geometrical irregularities. The Finite Volume Method (FVM) and WSGG method was applied to study

radiative heat transfer in the non-gray medium. Payan et al. [10-11] employed an inverse analysis to estimate the unknown heat flux distribution in two-dimensional enclosures with regular and irregular geometries.

The DOM combined with WSGG method was used to solve the Radiative Transfer Equation (RTE) in the non-gray participating media. The blocked-off procedure was also used to simulate the irregularities. A similarity solution for laminar boundary layer in a buoyancy induced flow over an isothermal, vertical wall in the presence of radiation was developed by Zeyghami and Rahman [12]. The effect of gray gas number in the weighted sum model is investigated on the calculation of the radiative heat transfer by Nenad et al. [13]. A computer code which solved the set of equations of the mathematical model describing the reactive two-phase turbulent flow with radiative heat exchange and with thermal equilibrium between phases inside the pulverized coal-fired furnace was used. The results of this investigation showed that if the weighted sum of the gray gases model was used, the complexity of the computer code and calculation time can be reduced by optimizing the gray gases number.

Chishty et al. [14] studied the importance of radiative heat transfer on the combustion and soot formation characteristics under nominal ECN Spray conditions. The effect of radiation absorption was found to be important and the typical radiation time scale was observed to overlap with the long injection duration, leading to a moderate influence on the temperature distribution. It was anticipated that NO_x formation rates were expected to be influenced by radiative heat transfer in a more pronounced manner. Full-Spectrumk-Distribution (FSK) look-up table was constructed by Wang et al. [15] for gas mixtures within a certain range of thermodynamic states for three species, i.e., CO₂, H₂O and CO. The k-distribution of a mixture was assembled directly from the summation of the linear absorption coefficients of three species. Results showed that, using the FSK look-up table can provide excellent accuracy compared to the exact results.

Keshtkar [16] studied radiative-conductive heat transfer using coupled DOM and energy equation in an enclosure with an isotherm obstacle and found good results. Ren et al. [17] studied radiative heat transfer numerically for reacting swirling flow in an industrial gas turbine burner operating at a pressure of 15 bar. The reacting field characteristics were computed by Reynolds-averaged Navier–Stokes (RANS) equations using the k- ϵ model with the Partially Stirred Reactor (PaSR) combustion model. It was found that radiation does not significantly alter the temperature level as well as CO₂ and H₂O concentrations. However, it has significant impacts on the NO_x levels at downstream locations. Yang et al. [18] numerically investigated radiation behaviours in small and large scale furnaces through refined radiative

property models, using the Full-Spectrum Correlated K (FSCK) model and Mie theory based data, compared with the conventional use of the Weighted Sum Of Grey Gases (WSGG) model and the constant values of the particle radiation properties. Ge et al. [19] investigated a magnetically tunable multiband NFRHT in a system of two suspended graphene sheets at room temperature. Shiue et al. [20] studied stable high-temperature thermal emission based on hot electrons (>2000 K) in graphene coupled to a photonic crystal nanocavity, which strongly modifies the EM LDOS.

Yin and Rosendahl [21] studied a new and complete set of Weighted Sum of Gray Gases Model (WSGGM), which is applicable to Computational Fluid Dynamics (CFD) modeling of both air–fuel and oxy–fuel combustion. A combined experimental and Large-Eddy Simulation (LES) study of molecular radiation was presented for combustion in a homogeneous pre-mixed spark-ignition engine by Henrion et al. [22]. A procedure based on two-step method was suggested to simplify time-consuming spectral radiative transfer calculations in open flames containing scattering particles by Dombrovsky et al. [23].

Atashafrooz et al. [24] investigated the interaction between non-gray radiation and forced convection in a laminar radiating gas flow over a recess including two backward and forward facing steps in a duct numerically. Fathi et al. [25] introduced a new approach for radiation heat flux calculations by coupling the discrete ordinates method with the Leckner global model. A line-by-line model with HITEMP2010 database was comprehensively investigated in one- and two- dimensional enclosures containing H2O/CO2/N2 by Chu et al. [26]. Boutoub et al. [27] used the Weighted-Sum-of-Gray-Gases (WSGG) model to investigate radiative heat transfer in non- gray media. The Finite Volume Method (FVM) was used to solve the radiative transfer equation. Furthermore, many researchers carried out similarity studies [28-34].

In the present study, thermal radiative heat transfer behavior of a non-gray gas is studied in a T-shape geometry in which the medium is considered to participate in the calculations. The RTE is solved using discrete ordinate method and also WSGGM is used to simulate the non-gray effects. Moreover, the Blocked-off method is used to simulate the irregular geometry. The effect of different radiative parameters on thermal behavior is studied. It is clear from the literature review that less attention was made in simulation of non-gray participating media with combination of Weighted Sum of Gray Gas Method (WSSGM) and Discrete Ordinate Method (DOM). Moreover, the other difference between present work and other references is using radiative heat transfer equation for a non-gray gas in a T-shape geometry that can be used to simulate complex engineering applications.

2 THEORETICAL ANALYSIS

2.1. Problem Description

According to “Fig. 1”, the geometric model used in this study is a T-shaped furnace with length L and height H.

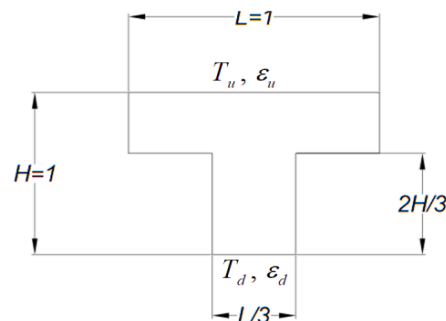


Fig. 1 The geometric model of T-shaped furnace.

The participating medium is air mixture with 20% of water vapor mole fraction supposed as a non-gray medium. The temperature of right wall including step surfaces is kept constant at T_r , left wall including step is at T_l , bottom wall including step is at T_d and the top wall is at T_u . The walls are assumed to emit and reflect diffusely with constant emissivity. Since the radiative thermal behavior is the dominant heat transfer mechanism, conduction and convection are considered to be neglected in the calculations.

2.2. Radiative Transfer Equation for a Gray Gas

The equation for radiative heat transfer (RTE) for a gray medium is presented as follows [35]:

$$\frac{dI}{ds} = s \cdot \nabla I(\vec{r}, \hat{s}) = -\beta(\vec{r})I(\vec{r}, \hat{s}) + S(\vec{r}, \hat{s}) \quad (1)$$

This equation indicates that change of intensity I takes place along the length of ds . The equation shows that change of intensity along a path is equal to the difference between the gained and lost energy. The term $-\beta(\vec{r})I(\vec{r}, \hat{s})$ is for attenuation and $S(\vec{r}, \hat{s})$ for augmentation. The extinction coefficient is given as follows:

$$\beta(\vec{r}) = \kappa(\vec{r}) + \sigma_s(\vec{r}) \quad (2)$$

Where $\kappa(\vec{r})$ is the absorption coefficient and $\sigma_s(\vec{r})$ is the scattering coefficient of radiant energy. Moreover, the source term in “Eq. (1)” can be obtained as follows:

$$S(\vec{r}, \hat{s}) = \kappa(\vec{r})I_b(\vec{r}) + \frac{\sigma_s(\vec{r})}{4\pi} \int_{4\pi} I(\vec{r}, \hat{s}') \Phi(\vec{r}, \hat{s}', \hat{s}) d\Omega' \quad (3)$$

The boundary condition for an opaque diffuse surface is:

$$I(r, \hat{s}) = \varepsilon(r) I_b(r) + \frac{\rho(r)}{\pi} \int_{\hat{n} \cdot \hat{s}' < 0} I(r, \hat{s}') |\hat{n} \cdot \hat{s}'| d\Omega' \quad (4)$$

The relation for radiative flux is as follows:

$$\nabla \cdot q = \kappa \left[4\sigma T^4 - \int_{4\pi} I(\vec{r}, \hat{s}) d\Omega \right] = \kappa \left[4\sigma T^4 - G(\vec{r}) \right] \quad (5)$$

Where, $G(\vec{r})$ is incident radiation:

$$G(\vec{r}) = \int_{4\pi} I(\vec{r}, \hat{s}) d\Omega \quad (6)$$

The total radiative heat flux onto a surface element is calculated by:

$$q \cdot \hat{n} = \int_{4\pi} I(\vec{r}, \hat{s}) \hat{n} \cdot \hat{s} d\Omega \quad (7)$$

2.3. Weighted Sum of Gray Gases Model (WSGGM)

Modeling of non-gray participating media has been conducted by several researchers. Smith [36] developed a module based on the concept of weighted sum of gray gases as follows:

$$\varepsilon = \sum_{i=0}^I a_{\varepsilon,i}(T) \left[1 - e^{-\kappa_i P S} \right] \quad (8)$$

Where, $a_{\varepsilon,i}$ denotes the emissivity weighting factors for the gray gas i and depend on gas temperature T . The quantity in the brackets in “Eq. (8)” is the i -th gray gas emissivity in which κ_i is the absorption coefficient, P is partial pressure and S is cross path length or thickness of gas layer. For a mixture of gas, P is the summation of partial pressures of absorbing gases. The weighting factor $a_{\varepsilon,i}$ shows the fractional amount of black body energy in the spectral regions where gray gas with absorption coefficient of κ_i exists. Zero value for absorption coefficient is for $i=0$ to account for windows in the spectrum between spectral regions of high absorption. This gas is called “clear gas”. The total emissivity is an increasing function of partial pressure-path length product approaching unity in the limit. Therefore, the weighting factors must sum to unity and also must have positive values. The weighting factor for clear gas, i.e. for $i=0$, is defined as follows:

$$a_{\varepsilon,0} = 1 - \sum_{i=1}^I a_{\varepsilon,i} \quad (9)$$

Thus, i values of the weighting factors must be defined. A usual and simple representation of dependency of the

weighting factors to the temperature is a polynomial of order $j-1$, so that this relationship can be expressed as:

$$a_{\varepsilon,i} = \sum_{j=1}^J b_{\varepsilon,i,j} T^{j-1} \quad (10)$$

Where, $b_{\varepsilon,i,j}$, are the emissivity gas temperature polynomial coefficients which are evaluated by fitting Eq. (8) to a table of total emissivities. For I gray gases and $j-1$ polynomial order, $I-J$ coefficients should be calculated. For the total absorptivity, the irradiation temperature of surfaces surrounding the gas, T_s , must be also taken into consideration. Therefore, the absorptivity is calculated by:

$$\alpha = \sum_{i=0}^I a_{\alpha,i}(T, T_s) \left[1 - e^{-\kappa_i P S} \right] \quad (11)$$

Here the absorptivity weighting factors $a_{\alpha,i}$ are also function of the surface irradiation temperature T_s . The summation of all weighting factors must be equal to unity and should all be positive. For $i=0$, the weighting factor is:

$$a_{\alpha,0} = 1 - \sum_{i=1}^I a_{\alpha,i} \quad (12)$$

The relation between weighting factors of gas and irradiation temperatures is expressed by polynomials of orders $j-1$ and $k-1$, as follows:

$$a_{\alpha,i} = \sum_{j=1}^J \left[\sum_{k=1}^K c_{\alpha,i,j,k} T_s^{k-1} \right] T^{j-1} \quad (13)$$

Where, $c_{\alpha,i,j,k}$ are the absorptivity polynomial coefficients. The number of coefficients that should be calculated for total absorptivity is equal to $I \times J \times K$.

2.4. Modification of General RTE Coupled with WSGGM

If the radiation heat transfer is modeled with one gray gas, the general integral-differential RTE is valid but in the case of non-gray media using WSGGM, more than one gray gas should be considered in the simulation and therefore, the RTE should be linked with WSGGM and as a result, a set of RTE's is derived. The modified RTE for a non-gray gas, can be written as follows:

$$\frac{dI_i(\vec{r}, \hat{s})}{ds} = \hat{s} \cdot \nabla I_i(\vec{r}, \hat{s}) = -\beta_i(\vec{r}) I_i(\vec{r}, \hat{s}) + a_{\varepsilon,i}(T) \kappa_i(\vec{r}) I_b(\vec{r}) + \frac{\sigma_s(\vec{r})}{4\pi} \int I_i(\vec{r}, \hat{s}') \varphi(\hat{s}', \hat{s}) d\Omega' \quad (14)$$

In “Eq. (14)”, $a_{\varepsilon,i}(T)$ is the emissivity weighting factor which was explained. The physical meaning of the weighting factor $a_{\varepsilon,i}(T)$ is the fractional amount of black-body energy in the regions of spectrum where gray gas have absorption coefficient κ_i . As the radiation energy is expressed by WSGGM, the boundary condition for a non-gray gas, and an opaque diffuse surface is expressed as follows:

$$I_i(\vec{r}_w, \hat{s}) = \varepsilon(\vec{r}_w) I_b(\vec{r}_w) a_{\varepsilon,i}(T, T_s) + \frac{\rho(\vec{r}_w)}{\pi} \int_{n \cdot \hat{s} > 0} I_i(\vec{r}_w, \hat{s}') (\hat{n} \cdot \hat{s}') d\Omega' \quad (15)$$

Using WSGGM, the total radiative energy which is transferred via total number of gray gases (I), can be calculated by the summation of left and right hand sides of “Eq. (14)” for all gray gasses:

$$\sum_{i=1}^I \frac{dI_i(\vec{r}, \hat{s})}{ds} = - \sum_{i=1}^I \beta_i(\vec{r}) I_i(\vec{r}, \hat{s}) + \sum_{i=1}^I a_{\varepsilon,i}(T) \kappa_i(\vec{r}) I_b(\vec{r}) + \sum_{i=1}^I \frac{\sigma_s(\vec{r})}{4\pi} \int I_i(\vec{r}, \hat{s}') \varphi(\hat{s}', \hat{s}) d\Omega' \quad (16)$$

In this equation, when $I=1$, only one gray gas is considered and “Eq. (16)” is simplified to “Eq. (1)” which is valid for monochromatic gas. Moreover, the total incident radiation receiving in all directions for a non-gray gas is equal to the sum of incident radiations for all of the gray gases and is expressed as follows:

$$G_{tot}(\vec{r}) = \sum_{i=1}^I G_{g,i}(\vec{r}) = \sum_{i=1}^I \int_{4\pi} I_{g,i}(\vec{r}, \hat{s}) d\Omega \quad (17)$$

Moreover, for all gray gases, the total radiative heat flux in the direction of the unit vector \hat{i} is the summation of heat fluxes for each of the gray gases in the direction of the unit vector \hat{i} which can be expressed as follows:

$$q_{n,tot}(\vec{r}) = \sum_{i=1}^I q_{n,g,i}(\vec{r}) = \sum_{i=1}^I \int_{4\pi} I_{g,i}(\vec{r}, \hat{s}) \hat{n} \cdot \hat{s} d\Omega \quad (18)$$

In addition, the total divergence of the radiative heat flux is calculated by the summation of the divergences for each of the gray gases which is expressed as follows:

$$\nabla \cdot q_{tot} = \sum_{i=1}^I \nabla \cdot q_{g,i} = \sum_{i=1}^I \kappa_{g,i} [4\pi a_{\varepsilon,i}(T) I_b(\vec{r}) - G_{g,i}(\vec{r})] \quad (19)$$

2.5. The Blocked-Off Method

In the present work, the blocked-off region method is used coupled with the DOM to handle T-shaped furnace. This procedure is suitable for irregular geometries using Cartesian coordinate’s formulation. By using the concept of blocked-off method, the region is divided into two parts: active and inactive or blocked-off regions. The region where solutions are calculated is known as the active region and the residual part is known as the inactive or the blocked-off region. In “Fig. 2”, T-shaped furnace is presented to show how it is treated to simulate from a rectangular geometry.

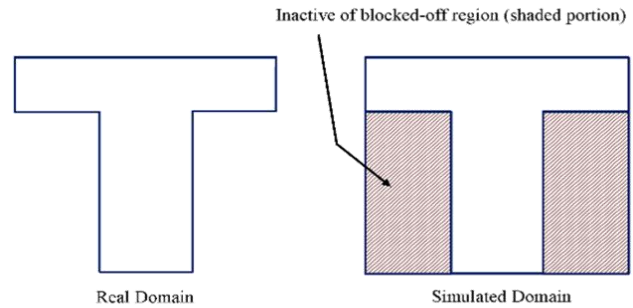


Fig. 2 Sample of T-shaped geometry.

The calculation is carried out over the whole domain, except inactive regions. Therefore, the magnitude of the independent variables such as temperature and intensity is set to be equal to zero at the cells of the blocked-off regions.

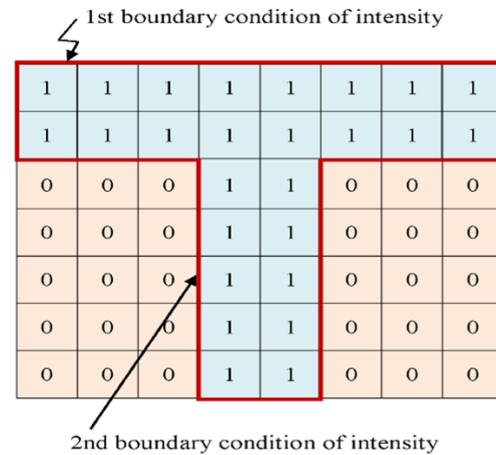


Fig. 3 Discretized domain.

As illustrated in “Fig. 3”, the simulated zone is discretized into several control volumes. The active control volumes are intended as one (1) and blocked-off parts is intended as zero (0). The magnitude of quantities that stay on the inactive region at the control volumes are set to zero value. Using the blocked-off method, additional boundary conditions should be defined as the second boundary conditions for those real boundaries,

which are due to the inserting of irregular geometry into the rectangular shape and consequently the real boundaries are located inside the computational domain. Depending on the shape of the geometry, in the computational code, a boundary condition file should be considered containing the control volumes adjacent to internal boundaries which are in the active region.

2.6. Discrete Ordinate Method (DOM)

By using DOM, “Eq. (14)” is solved for a set of 6 different directions, $s_i = 1, 2, 3, 4, 5, 6$ and the integrals over direction are replaced by numerical quadrature as follows:

$$\int_{4\pi} f(\hat{s}) d\Omega \approx \sum_{i=1}^n w_i f(\hat{s}_i) \tag{20}$$

Where, w_i are the quadrature weights associated with the directions s_i , thus, the “Eq. (14)” can be approximated by a set of 6 equations as follows:

$$\hat{s} \cdot \nabla I_i(\hat{r}, \hat{s}) = -\beta_i(\hat{r}) I_i(\hat{r}, \hat{s}) + a_{e,i}(T) \kappa_i(\hat{r}) I_b(\hat{r}) + \frac{\sigma_s(\hat{r})}{4\pi} \sum_{j=1}^n w_j I_i(\hat{r}, \hat{s}') \varphi(\hat{s}', \hat{s}) \quad i = 1, 2, \dots, 6 \tag{21}$$

In which the boundary conditions are:

$$I_i(r_\omega, \hat{s}) = \varepsilon(r_\omega) I_b(r_\omega) a_{a,i}(T, T_s) + \frac{\rho(r_\omega)}{\pi} \sum_{n,s_j < 0} w_j I_i(r_\omega, \hat{s}_j) |\hat{n} \cdot \hat{s}_j|, \quad \hat{n} \cdot \hat{s}_j > 0 \tag{22}$$

In multidimensional Cartesian coordinates, by using direction $\hat{s}_i = \xi_i \hat{i} + \eta_i \hat{j} + \mu_i \hat{k}$, Eq. (21) becomes:

$$\xi_i \frac{\partial I_i}{\partial x} + \eta_i \frac{\partial I_i}{\partial y} + \mu_i \frac{\partial I_i}{\partial z} + \beta I_i = \beta S_i \tag{23}$$

Where S_i is radiative source function and is expressed as follows:

$$S_i = (1 - \omega) a_{e,i}(T) I_b + \frac{\omega}{4\pi} \sum_{j=1}^n w_j I_j \tag{24}$$

The boundary condition along each surface is expressed as follows:

$$I_i = \frac{J_w}{\pi} = \varepsilon I_{bw} a_{a,i}(T, T_s) + \frac{1 - \varepsilon}{\pi} \sum w_j I_j |\xi_j| \tag{25}$$

A general two-dimensional control volume is shown in “Fig. 4”.

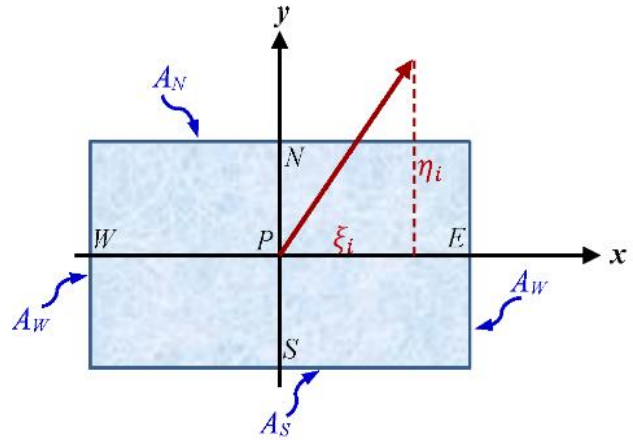


Fig. 4 A general two-dimensional control volume.

The volume element has four face areas A_W and A_E (in the x direction), and A_N and A_S (in the y direction) which can be calculated as follow:

$$\begin{aligned} A_{EW} &= (1 - \gamma_x) A_E + \gamma_x A_W, \\ A_{NS} &= (1 - \gamma_y) A_N + \gamma_y A_S \end{aligned} \tag{26}$$

where : $1/2 < \gamma_x, \gamma_y < 1$

The finite volume formulation of “Eq. (23)” is obtained by integrating it over a volume element:

$$\begin{aligned} \xi_i \int_S^N \int_E^W \frac{\partial I_i}{\partial x} dx dy + \eta_i \int_E^W \int_S^N \frac{\partial I_i}{\partial y} dx dy + \\ \int_E^W \int_S^N \beta I_i dx dy = \int_E^W \int_S^N \beta S_i dx dy \end{aligned} \tag{27}$$

Knowing the value of intensity at the left and bottom edges of control volume, the value of intensity at the cell center (P) can be found as follows:

$$\begin{aligned} I_{pi} &= \gamma_y I_{Ni} + (1 - \gamma_y) I_{Si} \\ &= \gamma_x (I_{Ei}) + (1 - \gamma_x) I_{Wi} \end{aligned} \tag{28}$$

By substituting “Eqs. (26) and (27)” in “Eq. (28)”, the simplified form of the “Eq. (28)” can be obtained as follows:

$$I_{pi} = \frac{\beta V S_{pi} + \xi_i A_{EW} I_{Wi} / \gamma_x + \eta_i A_{NS} I_{Si} / \gamma_y}{\beta V + \xi_i A_E / \gamma_x + \eta_i A_N / \gamma_y} \tag{29}$$

3 METHOD OF SOLUTION AND VALIDATION

The solution algorithm has been presented in “Fig. 5”.

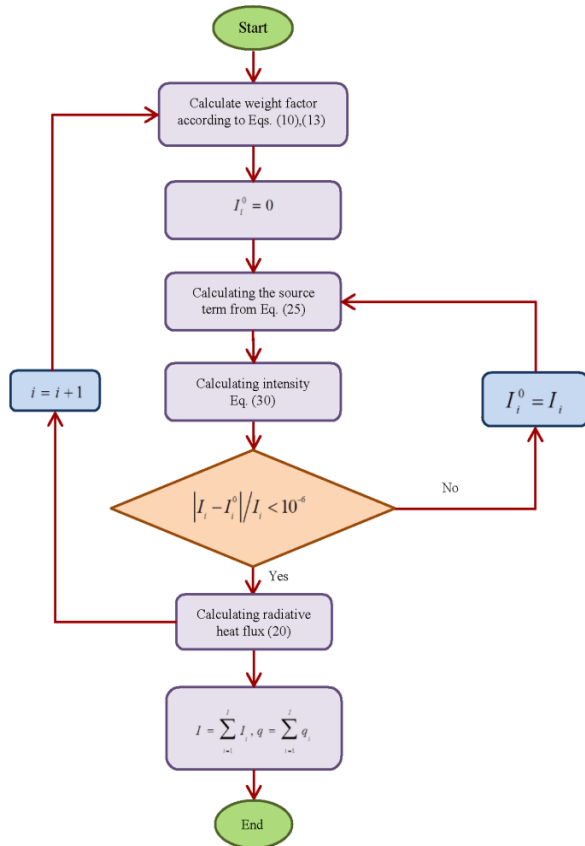


Fig. 5 Flowchart of non-gray algorithm solution.

To show the validity and the accuracy of the current method, several test problems have been compared with the available results of the literature. First, a test case is presented to show the validity of DOM method for gray medium. Second, a test case is given to show the validity of the blocked-off method in 2D geometry and the third one is given to show the validity of WSGGM method for non-gray medium.

Test problem 1: DOM method for gray medium

Figure 6 shows an enclosure containing cold emitting-absorbing medium, where the walls are black and cold except surface 1 which is black and hot.

The scattering coefficient is equal to 1 ($\sigma_s = 1$) and absorption coefficient is considered to be zero ($\kappa = 0$).

Figure 7 shows the radiative heat flux on the surface 1. This problem has been solved by S_2, S_4, S_6, S_8 approximation and compared with the results of Fiveland [37]. Figure 7 shows good consistency between the present results and those has been presented in ref. [37]. It can be found from “Fig. 7” that by increasing the ordinates, the

accuracy of results increases but on the other hand, due to the increase of calculations, the computational cost also increases. Therefore, in this paper the S_6 approximation has been chosen for high accuracy and less computational cost.

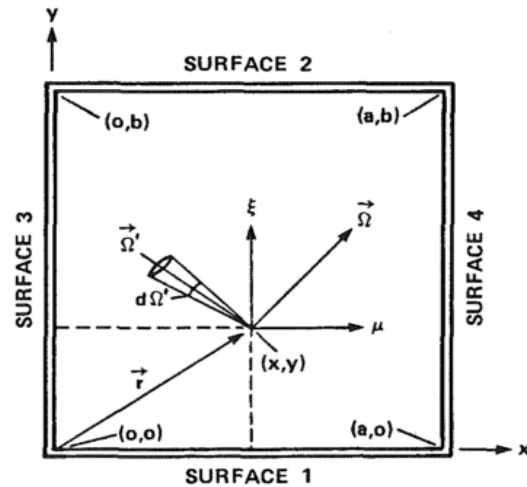


Fig. 6 The geometry of test problem 1.

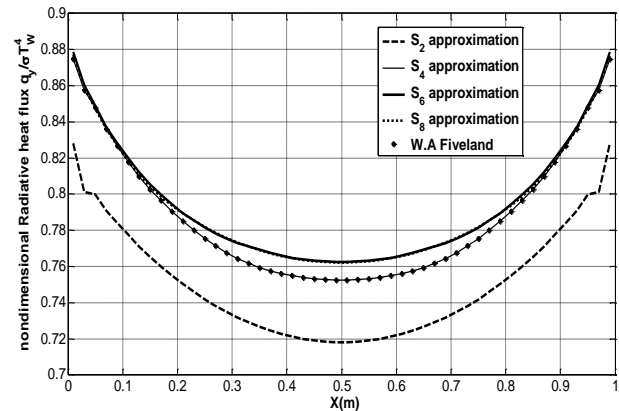


Fig. 7 Radiative heat flux on the bottom wall.

Test problem 2: Blocked-off method

As an irregular geometry, a square enclosure containing a cold emitting-absorbing media is considered which has been shown in “Fig. 8”, where the walls are black and cold except boundary 1 which is black and hot. The scatter coefficient is considered to be equal to 2 ($\sigma_s = 2$) and absorption coefficient is 0.5 ($\kappa = 0.5$). Figure 9 shows the comparison of solution with blocked-off region. Figure 9 shows the radiative heat flux on the bottom surface. The results obtained with the step scheme ($\gamma_x = \gamma_y = 1$) have been compared with those presented by Talukdar [3]. It is seen in “Fig. 9”, there is good consistency between present result and the results of ref. [3].

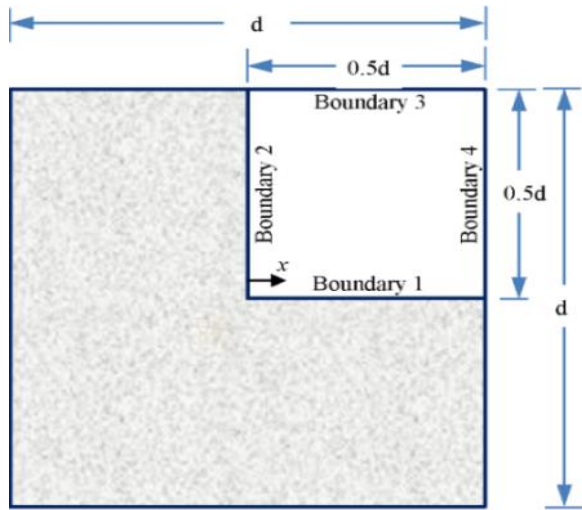


Fig. 8 The geometry of test problem 2.

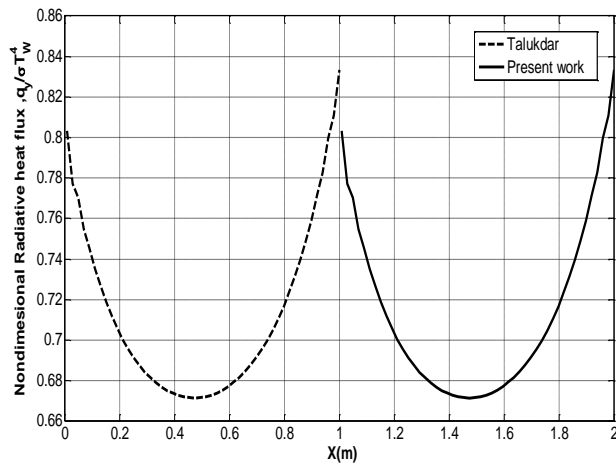


Fig. 9 Radiative heat flux on the bottom wall.

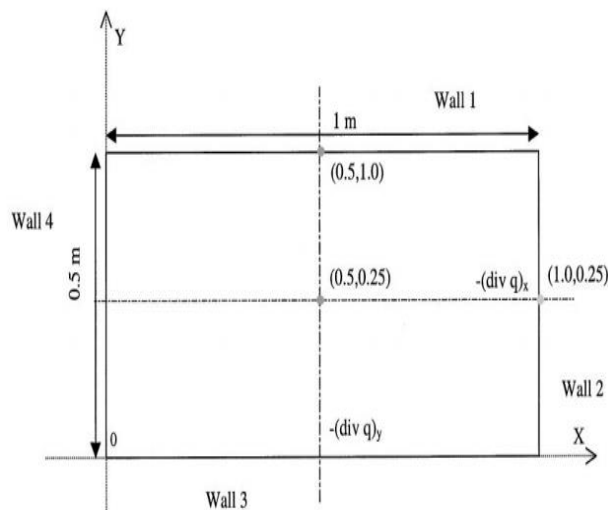


Fig. 10 Schematic of test problem 3.

Test problem 3: WSGGM for non-gray medium

The schematic of an enclosure containing 20 percent of isotropic H₂O has been shown in “Fig. 10” where the walls are cold black and the temperature of the medium is 1000 K. This problem has been studied by Goutiere [38] using several methods. In the present work, using WSSGM and the necessary coefficients from Smith [36], the obtained results have been presented in “Fig. 11”. Moreover, it is seen from this figure that the centerline divergence profile is in good agreement with those that has been presented in reference [38].

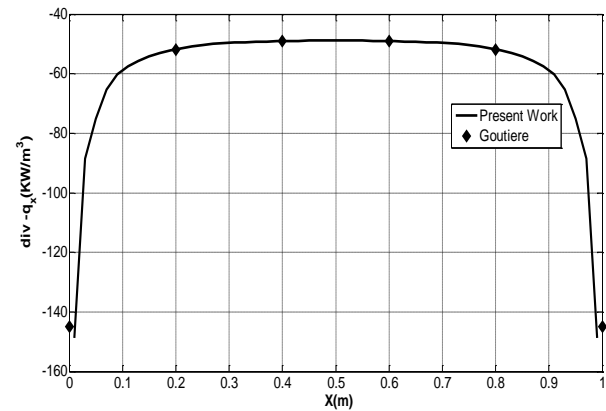


Fig. 11 Divergence of heat transfer at center line along x-direction.

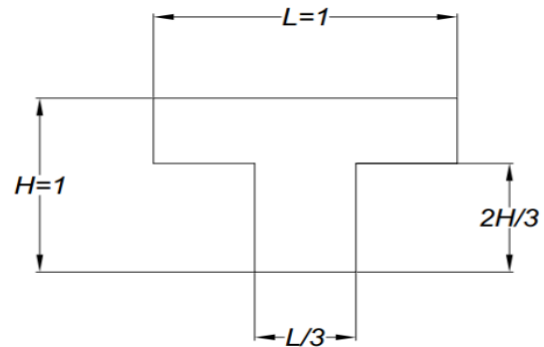


Fig. 12 Schematic of a T-shaped enclosure.

4 RESULTS AND DISCUSSION

In this section, the blocked-off region procedure is applied to a two-dimensional T-shaped enclosure shown in “Fig. 12”. All walls are black and cold and the medium is containing 20 percent of H₂O at 1000 K. The medium is assumed as non-gray gas in which the necessary radiative parameters are obtained from the study of Smith. Moreover, the WSGGM procedure is used to simulate the non-gray medium. The computations are performed by using 100×100 control volumes. Figure 13 shows that by

increasing the scattering coefficient, the radiative heat flux varies non-uniformly on the bottom walls. As it can be seen, the radiative heat flux decreases on the middle bottom wall and also on the wings of the T-part and increases on the other parts which is due to the irregular shape of the furnace.

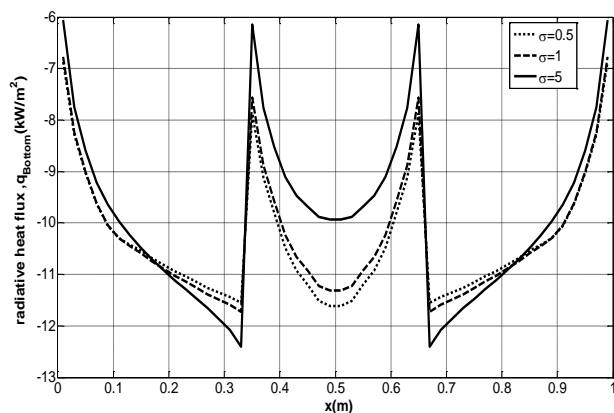


Fig. 13 Radiative heat flux at the bottom wall with non-gray medium for different scattering coefficients.

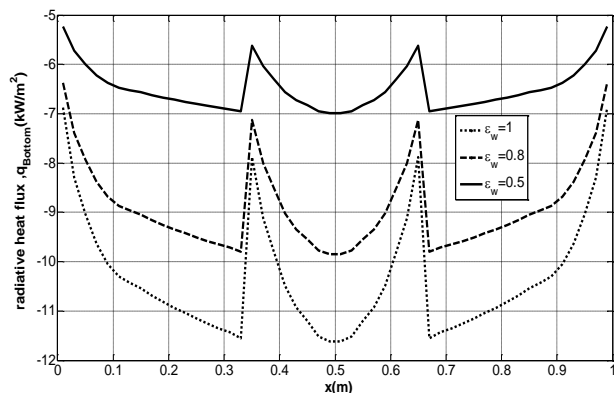


Fig. 14 Radiative heat flux at the bottom wall with non-gray medium for different wall emissivity.

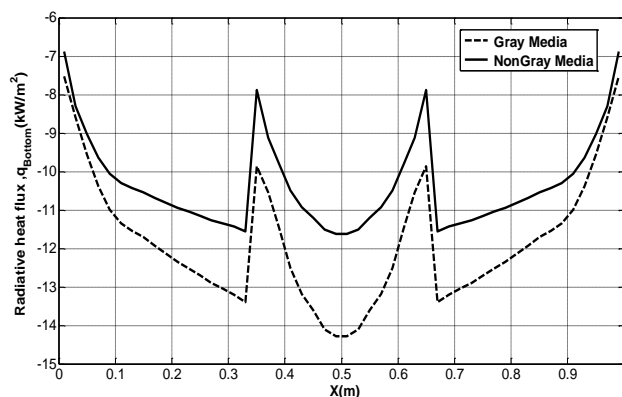


Fig. 15 comparison of Radiative heat flux at the bottom wall between gray and non-gray medium for $\sigma_s = 0.5$.

Furthermore, as expected, when scattering coefficient increases, more radiation is scattered in the medium and therefore less heat flux reaches the walls such that by increasing scattering coefficient from 1.0 to 5.0, the incident radiative heat flux decreases up to 15% in some parts of bottom wall. The effect of the wall emissivity on radiative heat flux is demonstrated in “Fig. 14”. This figure shows that by increasing the wall emissivity, the incident heat flux on the bottom wall decreases. This behavior is due to this fact that when wall emissivity increases, the wall behaves as a black one and therefore more heat flux is absorbed. Moreover, it should be mentioned that negative values of the wall heat flux show the incident heat flux to the wall. Figure 14 shows that by increasing wall emissivity from 0.5 to 1.0, wall heat flux increases more than 60%.

In “Fig. 15”, the obtained results are compared for gray and non-gray medium with scattering coefficient of $\sigma_s = 0.5$. As it is seen, there is a considerable difference between two assumptions. For a better comparison, the maximum error of radiative heat flux between gray and non-gray medium is presented in “Table 1”. As it can be seen from this table, by increasing the temperature, the maximum error strongly increases which indicates that in many engineering problems, the gray medium assumption leads to great error in results.

Table 1 Comparison of maximum error in different temperatures between gray and non-gray medium

Temperature (K)	Error (%)
1400	40.85
1000	17.73
800	5.0
500	0.13

5 CONCLUSIONS

In this work, the blocked-off method was used for handling of radiation heat transfer in T-shaped furnace and coupled with DOM and WSGGM algorithms. The results show that when scattering coefficient increases, more radiation is scattered in the medium and therefore less heat flux reaches the walls such that by increasing scattering coefficient from 1.0 to 5.0, the incident radiative heat flux decreases up to 15% in some parts of bottom wall. Moreover, the results show that by increasing wall emissivity from 0.5 to 1.0, wall heat flux increases more than 60%. Furthermore, it is seen that by increasing the temperature, the maximum error strongly increases which indicates that in many engineering problems, the gray medium assumption leads to great error in results.

6 NOMENCLATURE

a_α	Absorptivity weighting factors
ϵ	Emissivity weighting factors
b_ϵ	Emissivity polynomial coefficients
c_α	Absorptivity polynomial coefficients
E	Emissive power, W/m^2
G	Incident radiation, W/m^2
I	Radiation intensity, $W/m^2 \cdot sr$ or number of gray Gas components
J	Number of temperature polynomials coefficients
K	Number of irradiation polynomials coefficients
L	Length, m
n	Unit vector normal to the surface or number
P	Pressure, Pa
Q	Heat flux, W/m^2
S	Source term, W/m^3 or path length, m

Greek symbols

β	Extinction coefficient, $1/m$
ϵ	Emissivity of a surface
κ	Absorption coefficient, $1/m$
σ	Stefan-Boltzmann constant
σ_s	Scattering coefficient, $1/m$
ω	Scattering albedo

Subscripts

b	Black body
g	Gas
i	Gray gas

REFERENCES

- [1] Sakami, M., Charette, A., Application of a Modified Discrete Ordinates Method to Two-Dimensional Enclosures of Irregular Geometry, *Journal of Quantitative Spectroscopy & Radiative Transfer*, Vol. 64, 2000, pp. 275-298.
- [2] Koo, H. M., Goutière, R. V., Le, V., and Song, T. H., Comparison of Three Discrete Ordinates Methods Applied to Two-Dimensional Curved Geometries, *International Journal of Thermal Sciences*, Vol. 42, 2003, pp. 343-359.
- [3] Talukdar, P., Discrete Transfer Method with The Concept of Blocked-Off Region for Irregular Geometries, *Journal of Quantitative Spectroscopy & Radiative Transfer*, Vol. 98, 2006, pp. 238-248.
- [4] Borjinia, M. N., Guedri, K., and Said, R., Modeling of Radiative Heat Transfer in 3d Complex Boiler with Non-Gray Sooting Media, *Journal of Quantitative Spectroscopy & Radiative Transfer*, Vol. 105, 2007, pp. 167-179.
- [5] Han, S. H., Baek, S. W., and Kim, M. Y., Transient Radiative Heating Characteristics of Slabs in A Walking Beam Type Reheating Furnace, *International Journal of Heat and Mass Transfer*, Vol. 52, 2009, pp. 1005-1011.
- [6] Jang, J. H., Lee, D. F., Kim M. Y., and Kim, H. G., Investigation of the Slab Heating Characteristics in A Reheating Furnace with The Formation and Growth of Scale On the Slab Surface, *International Journal of Heat and Mass Transfer*, Vol. 53, 2010, pp. 4326-4332.
- [7] Keshtkar, M. M., Gandjalikhan Nassab, S. A., Theoretical Analysis of Porous Radiant Burners Under 2-D Radiation Field Using Discrete Ordinates Method, *Journal of Quantitative Spectroscopy & Radiative Transfer*, Vol. 110, 2009, pp. 1894-1907.
- [8] Ansari, A. B., Gandjalikhan Nassab, S. A., Study of Laminar Forced Convection of Radiating Gas Over an Inclined Backward Facing Step Under Bleeding Condition Using the Blocked-Off Method, *ASME, Journal of Heat Transfer*, Vol. 133, 2011, pp. 72-83.
- [9] Abbassi, M. A., Guedri, K., Borjini, M. N. Halouani, K., and Zeghmami, B., Modeling of Radiative Heat Transfer in 2D Complex Heat Recuperator of Biomass Pyrolysis Furnace: A Study of Baffles Shadow and Soot Volume Fraction Effects, *International Journal of Physical, Nuclear Science and Engineering*, Vol. 8, No. 2, 2014, pp. 119-129.
- [10] Payan, S., Hosseini Sarvari, S. M., and Behzadmehr, A., Inverse Boundary Design Radiation Problem Within Combustion Enclosures with Absorbing-Emitting Non-Gray Media, *Numerical Heat Transfer, Part A: Applications*, Vol. 65, 2014, pp. 1114-1137.
- [11] Payan, S., Farahmand, A., and Hosseini Sarvari, S. M., Inverse Boundary Design Radiation Problem with Radiative Equilibrium in Combustion Enclosures with PSO Algorithm, *International Communications in Heat and Mass Transfer*, Vol. 68, 2015, pp.150-157.
- [12] Zeyghami, M., Rahman, M. M., Analysis of Combined Natural Convection and Radiation Heat Transfer Using a Similarity Solution, *Energy Research Journal*, Vol. 6, No. 2, 2015, pp. 64- 73.
- [13] Nenad, D. J., Srdjan, V., Ivan, D., and Aleksandar, R., Monte Carlo Simulation for Radiative Transfer in a High-Pressure Industrial Gas Turbine Combustion Chamber, *Journal of Thermal Science*, Vol. 20, 2016, pp. 197- 206.
- [14] Chishty, M. A., Bolla, M., Hawkes, E., Pei, Y., and Kook, S., Assessing the Importance of Radiative Heat Transfer for ECN Spray a Using the Transported PDF Method, *International Journal of Fuels and Lubricants*, Vol. 9, No. 1, 2016, pp. 100-107.
- [15] Wang, C., Geb, W., and He, B., A Full-Spectrum K-Distribution Look-Up Table for Radiative Transfer in Nonhomogeneous Gaseous Media, *Journal of Quantitative Spectroscopy and Radiative Transfer*, Vol. 168, 2016, pp. 46-56.

- [16] Keshtkar, M. M., Amiri, B., Numerical Simulation of Radiative-Conductive Heat Transfer in an Enclosure with an Isotherm Obstacle, Heat Transfer Engineering, Vol. 39, No.1, 2018, pp. 72–83.
- [17] Ren, T., Modest, M. F., and Roy, S., Influence of the Gray Gases Number in the Weighted Sum of Gray Gases Model on the Radiative Heat Exchange Calculation Inside Pulverized Coal-Fired Furnaces, J. Eng. Gas Turbines Power, Vol. 140, No. 5, 2018, pp. 97- 108.
- [18] Yang, X., Clements, A., Szuhánszki, J., Huang, X., Farias O., Lia, J., Gibbins, J., Liu, Z., Zheng, C., Ingham, D., and Ma, L., Prediction of the Radiative Heat Transfer in Small and Large Scale Oxy-Coal Furnaces, Applied Energy journal, Vol. 211, 2018, pp. 523- 537.
- [19] Ge, L., Gong, K., Cang, Y., Luo, Y., Shi, X., and Wu, Y., Magnetically Tunable Multiband Near-Field Radiative Heat Transfer Between Two Graphene Sheets, Phys. Rev., Vol. 2, 2019, pp. 23- 37.
- [20] Shiue, R., Gao, Y., Tan, C., Peng, C., Zheng, J., Efetov, D., Kim, Y., Hone J., and Englund, D., Thermal Radiation Control from Hot Graphene Electrons Coupled to A Photonic Crystal Nanocavity, Nature Communications, Vol. 10, 2019, pp. 45- 56.
- [21] Yin, C., Rosendahl, L. A., New Weighted Sum of Gray Gases Model Applicable to Computational Fluid Dynamics (CFD) Modeling of Oxy–Fuel Combustion: Derivation, Validation, and Implementation, Energy Fuels, Vol. 24, No. 10, 2010, pp. 6275-6282.
- [22] Henrion, L., Gross, M. C., Fernandez, S. F., Paul, C., Kazmouz, S., Sick V., and Haworth, D. C., Characterization of Radiative Heat Transfer in A Spark-Ignition Engine Through High-Speed Experiments and Simulations, Oil & Gas Science and Technology, Vol. 74, No. 1, 2019, pp. 61-73.
- [23] Dombrovsky, A., Dembelele, S., Wend, J. X., and Sikic, I., Two-Step Method for Radiative Transfer Calculations in A Developing Pool Fire at The Initial Stage of Its Suppression by A Water Spray Leonid, International Journal of Heat and Mass Transfer, Vol. 127, Part B, 2018, pp. 717-726.
- [24] Atashafrooz, M., Gandjalikhan Nassab, R., Lari, K., Numerical Analysis of Interaction Between Non-Gray Radiation and Forced Convection Flow Over a Recess Using the Full-Spectrum K-Distribution Method, Heat and Mass Transfer, Vol. 52, No. 2, 2015, pp. 717-726.
- [25] Fathi, M., Hosseini, R., and Rahmani, M., Calculations of Non-Gray Gas Radiative Heat Transfer by Coupling the Discrete Ordinates Method with The Leckner Model in 3d Rectangular Enclosures, Heat and Mass Transfer, Vol. 52, No. 11, 2015, pp. 1-9.
- [26] Chu, H., Ren, F., and Zheng, S., A Comprehensive Evaluation of the Non Gray Gas Thermal Radiation Using the Line-By-Line Model in One- And Two-Dimensional Enclosures, Applied Thermal Engineering, Vol. 124, 2017, pp. 74-86.
- [27] Boutoub, A., Benticha, H., Non-Gray Radiation Analysis in Participating Media with the Finite Volume Method, Turkish Journal of Engineering and Environmental Sciences, Vol. 30, No. 3, 2006, pp. 183-194.
- [28] Jozaalizadeh, T., Toghraie, D., Numerical Investigation Behavior of Reacting Flow for Flameless Oxidation Technology of Mild Combustion: Effect of Fluctuating Temperature of Inlet Co-Flow, Energy, Vol. 178, No. 3, 2019, pp. 530-537.
- [29] Golestaneh, S. M., Toghraie, D., Separation of Particles from The Gas by Using of Cyclonic Separation in The Cyclotubes of Scrubber Installed in Gas Compressor Station, Powder Technology, Vol. 343, 2019, pp. 392-421.
- [30] Dabiri, S., Khodabandeh, E., Poorfar, Khoeini A., Mashayekhi, R., Toghraie, D., and Abadian Zade, A., Parametric Investigation of Thermal Characteristic in Trapezoidal Cavity Receiver for A Linear Fresnel Solar Collector Concentrator, Energy, Vol. 153, 2018, pp. 17-26.
- [31] Hemmat Esfe, M., Hajmohammad, H., Toghraie, D., Rostamian, H., Mahian O., and Wongwises, S., Multi-Objective Optimization of Nanofluid Flow in Double Tube Heat Exchangers for Applications in Energy Systems, Energy, Vol. 137, 2017, pp. 160-171.
- [32] Naderi, M., Ahmadi, G., Zarringhalam, M., Akbari, O., and Khalili, E., Application of Water Reheating System for Waste Heat Recovery in Ng Pressure Reduction Stations, with Experimental Verification, Energy, Vol. 162, 2018, pp. 1183-1192.
- [33] Ahmadi, G., Toghraie, D., and Akbari, O., Energy, Exergy and Environmental (3e) Analysis of The Existing Chp System in A Petrochemical Plant, Renewable and Sustainable Energy Reviews, Vol. 99, 2019, pp. 234-242.
- [34] Ahmadi, G., Toghraie, D., and Akbari, O. A., Technical and Environmental Analysis of Repowering the Existing Chp System in A Petrochemical Plant: A Case Study, Energy, Vol. 159, No. 3, 2018, pp. 937-949.
- [35] Modest, M. F., Radiative Heat Transfer, Second ed. 2003: Academic Press, 2003.
- [36] Smith, T. F., Shen, Z. F., and Friedman, J. N., Evaluation of Coefficients for The Weighted Sum of Gray Gases Model, ASME Journal of Heat Transfer, Vol. 104, 1982, pp. 602-608.
- [37] Fiveland, W. A., Discrete-Ordinates Solutions of the Radiativetransport Equation for Rectangular Enclosures, ASME, Journal of Heat Transfer, Vol. 106, 1984, pp. 699-706.
- [38] Goutierea, V., Liub, F., and Charette, A., An Assessment of Real-Gas Modelling in 2d Enclosures, Journal of Quantitative Spectroscopy & Radiative Transfer, Vol. 64, 2000, pp. 299-326.